land

MDPI

Article

Application of Remote Sensing and GIS in Monitoring Forest Cover Changes in Vietnam Based on Natural Zoning

An Nguyen [1,*], Vasily Kovyazin [1] and Cong Pham [2]

[1] Department of Land Management and Cadastres, Saint Petersburg Mining University, 21-Line, 2, St. Petersburg 199106, Russia; vfkedr@mail.ru
[2] Department of Land Resources and Real Estate Management, State University of Land Use Planning, Moscow 105064, Russia; phamchicongktqs@gmail.com
* Correspondence: annguyenthebeatles1997@gmail.com; Tel.: +7-(911)-086-16-74

Abstract: Forest cover changes monitoring in Vietnam has been conducted using remote sensing (RS) and geographic information systems (GIS). Given Vietnam's diverse climate, this study focused on the Thanh Hoa, Kon Tum, and Dong Nai provinces due to their distinct natural conditions and forest structures. Land cover was classified into five categories: broadleaf forests, mixed forests, shrubland/grassland/agricultural land, non-forested areas, and water bodies. RS data processing was performed using Google Earth Engine (GEE), with land cover classification conducted via the Random Forest algorithm. The findings revealed significant changes in forest cover between 2010 and 2020. In Thanh Hoa, broadleaf forests expanded by 51.15% (91,159 ha), while mixed forests declined by 19.68% (105,445 ha). Kon Tum experienced reductions in both broadleaf forests (20.05%, 26,685 ha) and mixed forests (4.06%, 20,501 ha). Meanwhile, Dong Nai recorded increases in broadleaf forests (29.15%, 23,263 ha) and mixed forests (12.17%, 20,632 ha). The study's reliability was confirmed by a Kappa coefficient of 0.81–0.89. To predict forest cover changes, two methods—the CA-Markov model and the MOLUSCE module—were compared. Results demonstrated that the MOLUSCE module achieved higher accuracy, with deviations from actual data of 1.61, 1.14, and 1.80 for Thanh Hoa, Kon Tum, and Dong Nai, respectively, whereas the CA-Markov model yielded larger deviations (8.79, 6.29, and 5.03). Future forest cover projections for 2030, generated using MOLUSCE, suggest significant impacts from agricultural expansion, deforestation, and restoration efforts on forest area. This study highlights the advantages of remote sensing and GIS for complex forest monitoring and sustainable management in Vietnam.

Keywords: remote sensing; forest resources; land monitoring; GIS technologies; digital elevation model

check for updates

Academic Editor: Alexandru-Ionuţ Petrişor

Received: 6 April 2025
Revised: 30 April 2025
Accepted: 7 May 2025
Published: 9 May 2025

Citation: Nguyen, A.; Kovyazin, V.; Pham, C. Application of Remote Sensing and GIS in Monitoring Forest Cover Changes in Vietnam Based on Natural Zoning. *Land* **2025**, *14*, 1037. https://doi.org/10.3390/land14051037

Copyright: © 2025 by the authors. Licensee MDPI, Basel, Switzerland. This article is an open access article distributed under the terms and conditions of the Creative Commons Attribution (CC BY) license (https://creativecommons.org/licenses/by/4.0/).

1. Introduction

Remote sensing (RS) and geographic information systems (GIS) have become indispensable tools for monitoring and managing forest resources worldwide, particularly in countries with complex terrains and diverse ecosystems such as Vietnam. In forest land inventories, laser scanning is used, while linear regression methods are employed for automating land valuation assessments [1]. Satellite systems enable the analysis of urban vegetation conditions [2]. In forest management in Russia and European countries, digitalization is considered a promising approach [3]. GIS technologies have been applied to establish protective zones around cultural heritage sites [4]. In Vietnam, complex terrain and climatic conditions limit the extent and scale of research. With a forest cover of 47.6%

and with most of the landscape being mountainous, traditional methods of forest land monitoring face significant limitations [5]. Field-based surveys are often time-consuming, labor-intensive, and hindered by accessibility challenges in remote or rugged areas. Furthermore, the country's diverse regional climate patterns and unpredictable natural disasters (including storms, floods, and prolonged droughts) consistently disrupt field data collection and verification efforts. Consequently, RS has emerged as the primary effective method for forest land monitoring [6]. Nonetheless, challenges remain in developing comprehensive methodologies that fully utilize available data sources and analytical techniques. Current approaches often demonstrate deficiencies in classification accuracy, temporal change detection, and the integration of environmental variables into land cover analysis models [7].

While previous studies have demonstrated the applicability of RS and GIS technologies in monitoring forest cover, many have relied primarily on spectral data, without integrating supplementary variables such as Digital Elevation Models (DEM), slope data, and socio-environmental factors [8]. These omissions can result in oversimplified models that inadequately capture the factors of forest cover change.

RS technology has become an important tool in Earth research, enabling the collection of information about the surface and atmosphere remotely through sensors mounted on satellites, aircraft, or drones [9]. With the ability to record multi-spectral, multi-spatial, and multi-temporal data, remote sensing provides a continuous data source that supports the monitoring of environmental changes with high accuracy. This technology is widely applied in various fields such as land cover mapping, forest monitoring, urban planning, disaster management, precision agriculture, and climate change research [10]. A key advantage of remote sensing is its ability to cover large areas, including those that are hard to reach, providing synchronized and continuous real-time data. It can also be integrated with GIS for in-depth spatial analysis. As a result, RS is playing an increasingly essential role in both scientific research and supporting evidence-based decision making [11].

GIS has revolutionized spatial analysis through its ability to integrate, process, and visualize multidimensional geographic data [12]. Modern GIS platforms, including ArcGIS, QGIS, and the Google Earth Engine (GEE) cloud computing platform, offer significant advantages for forest cover monitoring. ArcGIS stands out for its comprehensive analytical toolset, user-friendly interface, and robust data processing capabilities, making it well suited for professional organizations. GEE enables the processing of large volumes of satellite data with high computational efficiency, facilitates cloud-based pre-processing (e.g., cloud masking, atmospheric correction), and supports the integration of multiple data types, including topographic and socio-environmental layers [13]. Meanwhile, QGIS is a powerful, flexible, and cost-effective open-source solution.

The integration of RS data with GIS and machine learning algorithms enhances natural resource management by combining satellite data with ground-based measurements, climate indicators, and socio-economic factors [14]. RS also contributes to addressing transboundary environmental issues such as deforestation and habitat fragmentation.

The simulation and prediction of land cover changes have become critical components of forest resource management, particularly in dynamic environments. The CA-Markov model, combining cellular automata and Markov chain analysis, has been widely used to simulate land use and land cover transitions based on historical patterns. For example, in Ezhou City, China, the Markov-FLUS model was successfully applied to forecast multi-scenario land use changes and ecosystem service dynamics under the expansion of construction land [15]. Similarly, in the Cerrado/Atlantic forest ecotone of Brazil, Markov-based models contributed to understanding long-term land use and land cover change under the

advancement of agriculture [16]. These studies demonstrate the value of transition-based modeling frameworks in capturing land use trends over time.

However, the CA-Markov model relies exclusively on historical transition probabilities and assumes land cover change processes remain stationary over time. This approach cannot fully incorporate the influence of external factors. To overcome these limitations, new approaches, such as the MOLUSCE (Modules for Land Use Change Simulation) module integrated in QGIS, have been developed. MOLUSCE incorporates Artificial Neural Networks (ANNs) to model complex, nonlinear relationships between land cover changes and multiple environmental, socio-economic variables. These capabilities are crucial for enhancing the accuracy, scalability, and reproducibility of forest cover monitoring workflows [17]. The application of ANNs to complex forest ecosystems, such as in the Eastern Mediterranean region of Turkey, has shown potential for evaluating eco-friendly soil slope stabilization techniques for forest roads [18].

This study aims to address existing methodological limitations by developing an enhanced classification and prediction framework that integrates spectral, vegetative (NDVI), topographic (DEM, slope), climatic (temperature, precipitation) and anthropogenic (distance to road and urban centers) data. The Random Forest (RF) machine learning algorithm is used to classify land cover categories, and two predictive models—the CA-Markov model and the MOLUSCE module (based on Artificial Neural Networks, ANNs)—are compared to predict forest cover changes in three ecologically distinct provinces of Vietnam: Thanh Hoa, Kon Tum, and Dong Nai. By integrating diverse data sources and advanced modeling techniques, this research seeks to improve the robustness and accuracy of forest cover monitoring in Vietnam, contributing valuable insights for sustainable forest management and land use planning.

2. Materials and Methods

2.1. Study Areas

This study focuses on monitoring forest cover changes in three provinces: Thanh Hoa, Kon Tum, and Dong Nai, located in the northern, central, and southern regions of Vietnam, respectively.

Thanh Hoa is located in the North Central region of Vietnam, with geographical coordinates ranging from 19°18′ to 20°40′ north latitude and from 104°22′ to 106°05′ east longitude. The province features diverse topography, including lowlands, midlands, and mountainous areas, and has a tropical monsoon climate with abundant rainfall. Forest land occupies approximately 52% of the total natural area, primarily concentrated in the western mountainous districts such as Quan Son, Quan Hoa, and Muong Lat [19]. This forest resource plays a crucial role in environmental protection and the development of the forestry-based economy.

Kon Tum is located in the northern part of the Central Highlands of Vietnam, with geographical coordinates ranging from 13°55′ to 15°27′ north latitude and from 107°20′ to 108°32′ east longitude. The province is characterized by mountainous terrain and plateaus, with a tropical monsoon climate that varies significantly with altitude. Forest land accounts for over 60% of the total natural area, mainly concentrated in districts such as Dak Glei, Tu Mo Rong, and Kon Plong [20]. This forest resource plays a vital role in biodiversity conservation and the sustainable development of the forestry economy.

Dong Nai is located in the Southeast region of Vietnam, with geographical coordinates ranging from 10°30′ to 11°34′ north latitude and from 106°45′ to 107°35′ east longitude. The province features mainly low hills and semi-mountainous terrain, with a tropical monsoon climate characterized by two distinct seasons. Forest land accounts for approximately 29% of the total natural area, notably including the Dong Nai Biosphere Reserve and Nam Cat

Tien Forest [21]. The province's forest resources play a critical role in ecosystem protection, climate regulation, and the sustainable development of the forestry sector. The geographic location of study areas is illustrated in Figure 1.

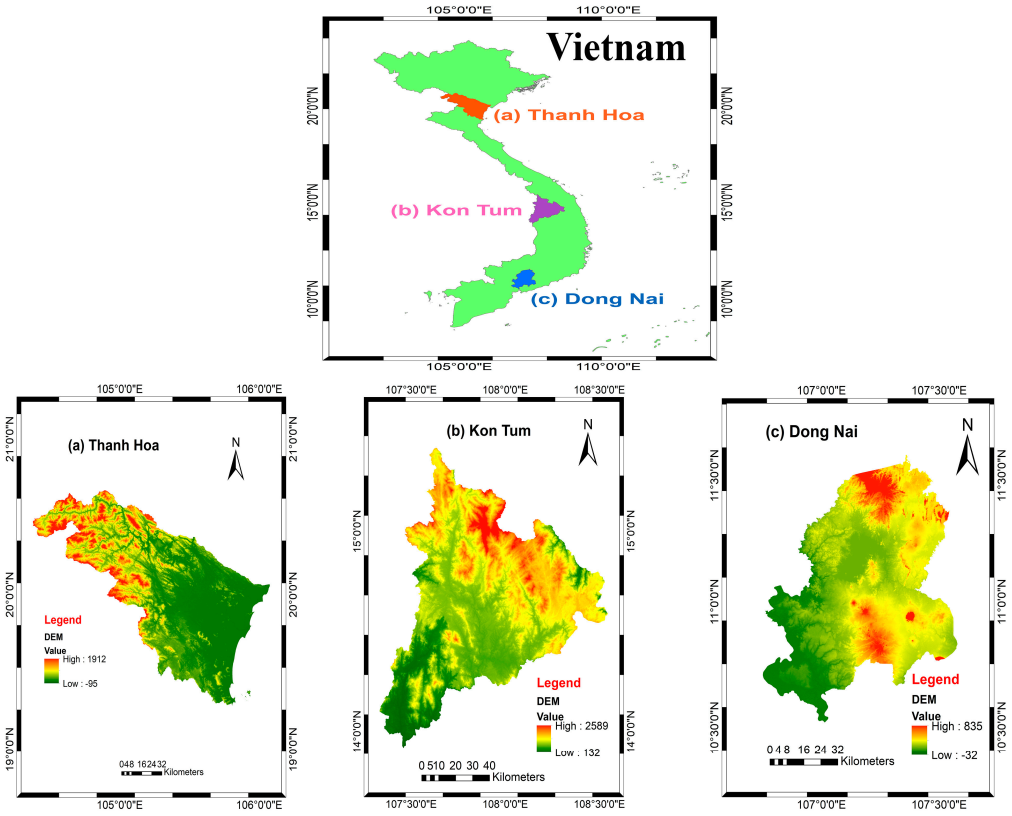


Figure 1. Study areas.

2.2. Data Collection

The data used for this study were collected from various sources, including satellite remote sensing data, Google Earth images, field maps, topographic data, distance to roads and urban centers, and regional-scale climatic variables.

Satellite images from Landsat 7 and Landsat 8, with a 30 m spatial resolution, were obtained from the United States Geological Survey (USGS), while Sentinel-2 satellite images with a 10 m resolution were sourced from the European Space Agency (ESA). Table 1 provides detailed information about the satellite images used in this study.

Topographic data consisted of Digital Elevation Models (DEMs) derived from the Shuttle Radar Topography Mission (SRTM) dataset, and slope data, with a spatial resolution of 30 m. The DEMs were processed in ArcGIS to generate slope layers, which were later used as supplementary variables in classification and prediction modeling (Figure 2). Distances to roads and urban centers were calculated from OpenStreetMap infrastructure data (accessed via OSMnx Python package, version 1.1.2) using geometries extracted in GeoJSON format. Regional-scale climatic variables, including annual precipitation and mean annual temperature, were obtained from the WorldClim v2 dataset at a spatial resolution of approximately 1 km. Google Earth Pro (version 7.3.6) images and field maps were used to improve the accuracy of land cover classification. Furthermore, pre-processing of the remote sensing data included cloud cover assessment, radiometric calibration, and atmospheric correction, all performed using the JavaScript API on the Google Earth Engine (GEE) code editor platform (updated as of November 2024).

Table 1. Satellite remote sensing data description and sources.

Year	Thanh Hoa	Kon Tum	Dong Nai	Data Parameters	Data Sources
2010	LE07 (T1_L2)	LE07 (T1_L2)	LE07 (T1_L2)	USGS Landsat 7 Level 2, Collection 2, Tier 1. Spatial resolution 30 m	United States Geological Survey (USGS)
2015	LC08 (T1_L2)	LC08 (T1_RT)	LC08 (T1_RT)	USGS Landsat 8 Level 2, Collection 2, Tier 1; Landsat 8 Collection 2 Tier 1 and Real-Time. Spatial resolution 30 m	United States Geological Survey (USGS)
2020	T48QXG/QWG/ QVH/QWH	LC08 (T1_RT)	T48PXT/PYT/ PXS/PYS	USGS Landsat 8 Collection 2 Tier 1 and Real-Time. Spatial resolution 30 m. Sentinel-2 MSI: MultiSpectral Instrument, Level-2A; Spatial resolution 10 m	United States Geological Survey (USGS); European Space Agency (ESA)

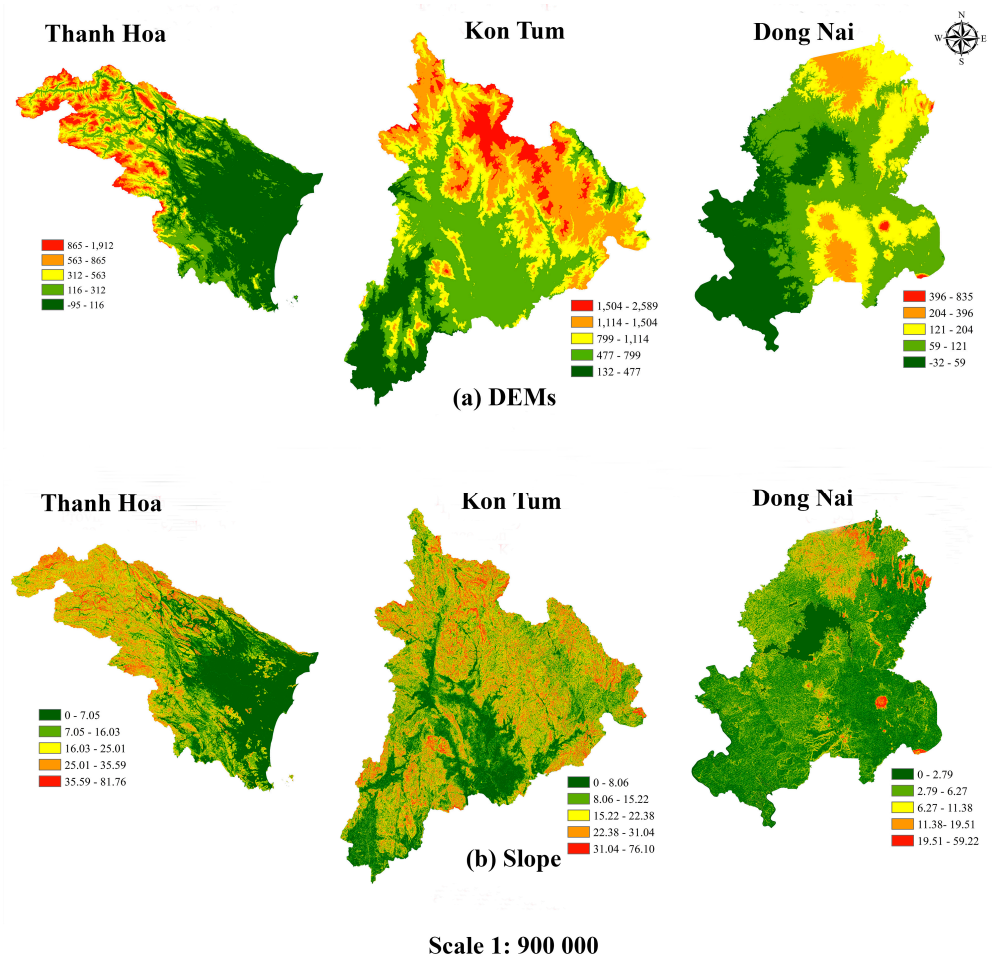


Figure 2. Topographic data.

2.3. Method

2.3.1. Land Cover Classification

Land cover classification was conducted using the Normalized Difference Vegetation Index (NDVI), spectral band combinations, Google Earth images, and field maps. On the GEE platform, the function ee.Image.normalizedDifference([x, y]), where x represents

the value of the near-infrared channel and y represents the value of the red channel, was employed to calculate NDVI for each province at different time points: 2010, 2015, and 2020. The NDVI served not only as a visualization tool but also as an input variable for the RF classifier, enhancing discrimination between forest types based on vegetation density. After calculation, the NDVI maps were integrated with the spectral bands and topographic layers to form a comprehensive multi-band image collection for each classification year. This integration enabled the RF model to simultaneously consider vegetation vigor (through NDVI), spectral signatures, and terrain characteristics when distinguishing between land cover categories [22].

Spectral band combinations, particularly the Red, Green, and Blue (RGB) and Color Infrared (NIR, red, and green) composites, were used during visual interpretation to aid the selection of training samples. These combinations allowed for more effective identification of land cover categories, particularly distinguishing dense broadleaf forests from mixed forests and agricultural lands [23].

Particular attention was paid to accurately distinguishing between mixed forests and broadleaf forests. Broadleaf forests typically exhibited higher NDVI values and more uniform canopy reflectance. In contrast, mixed forests—comprising a combination of deciduous and evergreen species—showed greater variability in spectral signatures, and slightly lower NDVI values due to seasonal leaf fall or species heterogeneity. These biophysical distinctions were critical for training sample selection: reference samples for broadleaf forests were selected in areas with consistently high NDVI values (>0.7) across multiple dates and with lower variability in spectral bands; samples for mixed forests were chosen from areas with moderate NDVI values (0.5–0.7) and more heterogeneous spectral reflectance. This sampling strategy ensured that the RF classifier could learn and differentiate forest types, thus improving classification performance in heterogeneous and mountainous environments.

Using the Random Forest algorithm, land cover was classified into five categories: (1) water bodies; (2) non-forested areas; (3) shrubland/grassland/agricultural land; (4) mixed forests; (5) broadleaf forests. Training data were generated through random sampling, guided by visual interpretation of satellite imagery, Google Earth data, and field maps. Approximately 200–250 sample points were collected for each land cover category. The dataset was divided into 70% for training and 30% for validation. The quality and representativeness of the samples directly influenced classification performance. Well-distributed, accurately labeled samples enabled the RF model to learn the unique spectral, vegetative, and topographic characteristics of each category more effectively. This was particularly important for distinguishing spectrally similar categories, such as mixed forests and broadleaf forests. The RF model was configured with 500 decision trees and used all available input features (spectral bands, NDVI, elevation, and slope). The Gini impurity index was employed for feature selection at each split. Classification accuracy was assessed using confusion matrices, with overall accuracy and the Kappa coefficient reported to evaluate the agreement between classified maps and reference data.

2.3.2. Forest Cover Changes Prediction

A. CA-Markov Model

Accurate predictions play a key role in decision-making processes aimed at the effective conservation and restoration of the country's forest resources. The CA-Markov model, which utilizes Markov transition matrices, is commonly applied to predict land use and land cover changes [24]. This widely used method models land cover transitions by analyzing the probabilities of change between different classes. Utilizing the CA-Markov

model, the area or state of land cover S(t + n) at a future time t + n is determined using the following equation:

$$S(t + n) = P^n \times S(t) \quad (1)$$

where

S(t): The state of land cover at the initial time t, represented as a column matrix indicating the area or proportion of each land cover class.

P: The Markov transition matrix, which defines the probability of transition from one land cover category to another over a given time period.

n: The number of time steps (forecasting period).

S(t + n): The predicted state of land cover at time t + n.

The initial state S(t) is typically represented as a column matrix, where each element Si(t) corresponds to the area or percentage of land cover type i at time t, as follows:

$$S(t) = \begin{bmatrix} S_1(t) \\ S_2(t) \\ S_3(t) \\ S_4(t) \\ S_5(t) \end{bmatrix} \quad (2)$$

where

$S_1(t)$: Area of broadleaf forests at time t.

$S_2(t)$: Area of mixed forests at time t.

$S_3(t)$: Area of shrubs, meadows and agricultural lands at time t.

$S_4(t)$: Area of unvegetated and non-forested lands at time t.

$S_5(t)$: Area of water fund lands at time t.

The CA-Markov model combines cellular automata (CA) and Markov chain analysis to simulate land cover transitions based on historical patterns. In this study, the transition probability matrices were generated using land cover classification results from 2010 and 2015. These classified maps served as the base data for transition analysis. The IDRISI TerrSet 2020 software was used to calculate the transition matrices and to project future land cover distributions. The CA component allowed spatial allocation of changes based on neighborhood rules, while the Markov chain component modeled the probability of transition between categories. The prediction accuracy of the CA-Markov model was evaluated by comparing the predicted 2020 land cover maps with the actual classified 2020 maps. Overall deviation percentages of predicted land cover areas were calculated for each province, providing quantitative measures of model performance.

The CA-Markov model offers several advantages, including simplicity, accessibility, the ability for long-term forecasting, and integration with spatial data [25]. Despite its benefits, the CA-Markov model is limited by its reliance on historical transition probabilities and its inability to incorporate external environmental or socio-economic factors. This study addresses these limitations by supplementing the prediction process with an ANN-based modeling approach that integrates a broader range of input variables influencing forest dynamics.

B. MOLUSCE Module

MOLUSCE module in Qgis software (version 2.18.10) works on the principle of an Artificial Neural Networks (ANNs) algorithm. ANNs are powerful machine learning algorithms designed to model complex, nonlinear relationships among multiple variables [26]. These networks can be trained on historical data, identify intricate relationships between multiple factors, and generate reliable forecasts. The method is based on simulating the

functioning of the human brain, where neurons are interconnected, forming responses and making decisions.

The fundamental equation for a hidden layer in an ANN is defined as follows:

$$y_i = f(\sum_{i=1}^{n} w_{ij} x_i + b_j) \quad (3)$$

where

x_i: Input features.

w_{ij}: Weight of the connection between input neuron i and hidden neuron j.

b_j: Bias term for neuron j.

y_i: Output of the hidden layer neuron j.

f: Activation function.

2.4. Structure of the ANN Algorithm

Input layer includes: land cover maps from 2010 and 2015 (classified using the RF algorithm); elevation and slope layers derived from the 30 m resolution SRTM DEM; distance to roads and urban centers, calculated from OpenStreetMap infrastructure data; regional-scale climatic variables, including annual precipitation and mean annual temperature, obtained from the WorldClim v2 dataset at a spatial resolution of approximately 1 km). Demographic data at high spatial resolution were not directly available; therefore, distance to roads and urban centers was used as proxy variables of anthropogenic impacts. All input layers were resampled to 30 m resolution to match the spatial resolution of the land cover maps, ensuring consistency across datasets.

The ANN model was trained using a supervised learning approach, where the land cover transitions between 2010 and 2015 served as the training target. The structure of the ANN consisted of an input layer, ten hidden layers using sigmoid activation functions, and an output layer predicting transition probabilities for each land cover category. The training dataset consisted of 1000 randomly selected points, stratified across land cover categories.

After training, the ANN algorithm was used to predict future land cover states based on the following equation:

$$Y = ANN\ (X) \quad (4)$$

where

X: set of input data.

Y: predicted results, representing the area or probability of land cover categories in the future.

Model accuracy was evaluated by comparing the predicted 2020 land cover maps with the actual classified 2020 maps. Accuracy assessment included calculating overall deviation percentages of predicted land cover areas for each province and Kappa coefficients using confusion matrices.

In the context of forest land monitoring, ANNs allow for the consideration of various factors, including climate, demographics, forest management policies, and socio-economic conditions. However, this method also has limitations: high demand for diverse data, including ecological and socio-economic indicators; and complex interpretation of results, making it difficult to isolate key factors influencing forecasts [27]. In this study, the lack of social and economic datasets was partially compensated by using distance-based proxy variables (e.g., distance to roads, urban centers). The model architecture, including the number of hidden layers and neurons, was optimized through a trial-and-error process to achieve a balance between model complexity and overfitting.

The research workflow is illustrated in Figure 3.

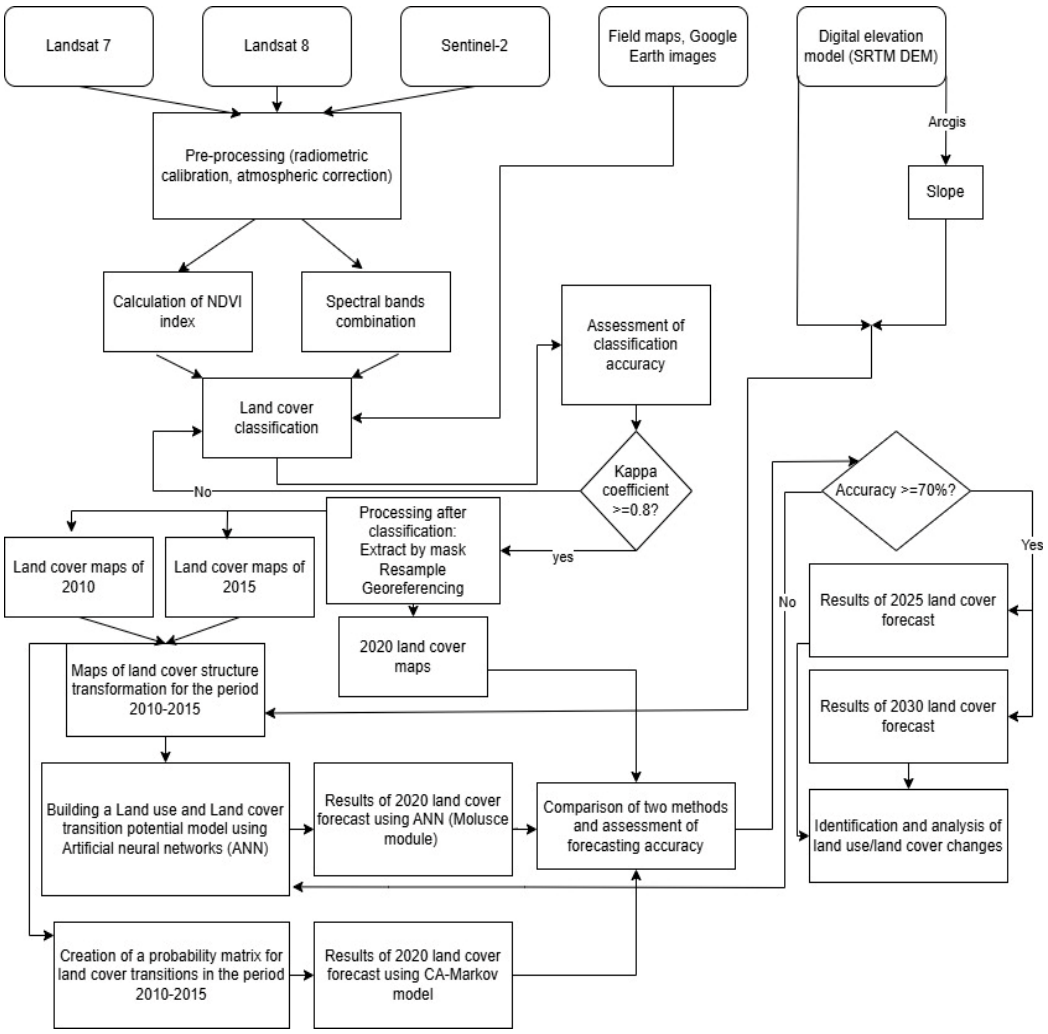


Figure 3. Research workflow.

3. Results

3.1. Forest Cover Changes in the 2010–2020 Period

The NDVI was calculated and displayed on the GEE interface. Green indicated areas with vegetation cover, with more intense shades of green corresponding to denser vegetation. In contrast, yellow represented non-vegetated areas or populated regions, with higher saturation reflecting greater population density. Water surfaces were depicted in white, as shown in Figure 4.

By integrating NDVI values with spectral band combinations and validating them using topographic data and Google Earth imagery, five land cover classes were identified in each province using the Random Forest algorithm. A confusion matrix was used to calculate classification accuracy and the Kappa coefficient. Table 2 presents high accuracy values and Kappa coefficients, indicating the reliability of the land cover classification results. Following classification, the data were processed in ArcGIS 10.8 using the WGS_1984_UTM_Zone_48N coordinate system, which facilitated the creation of land cover maps, as shown in Figure 5. The dynamics of various land cover categories are detailed in Table 3.

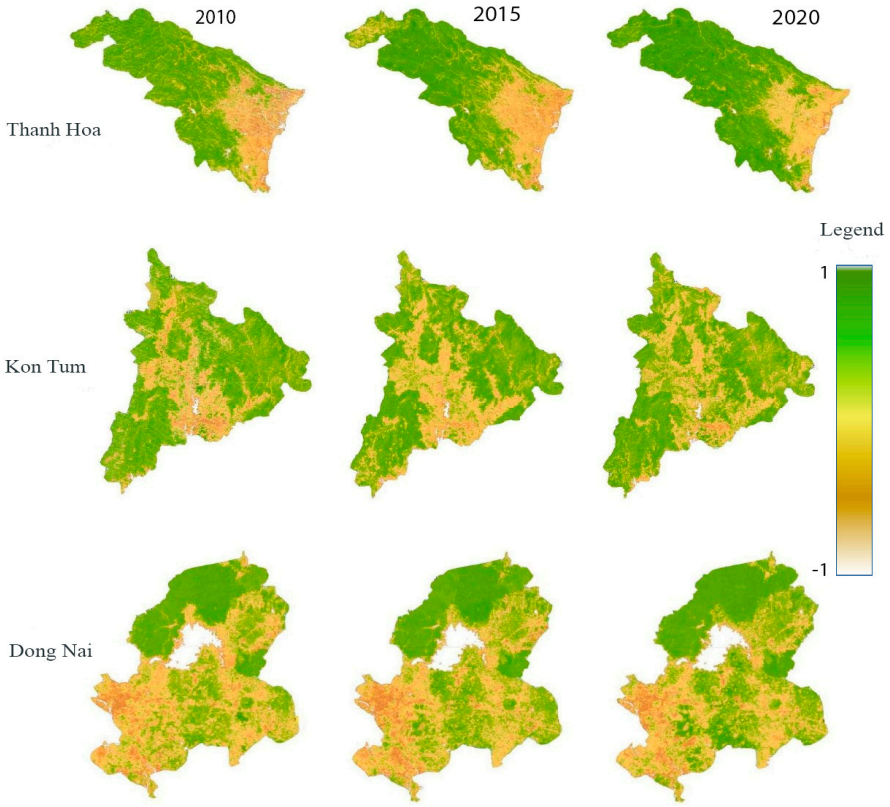


Figure 4. Visualization of NDVI values for the study areas.

Table 2. Accuracy assessment of land cover classification.

Research Objects	Year	Overall Accuracy	User's Accuracy	Producer's Accuracy	Kappa Coefficient
Thanh Hoa	2010	0.86	0.89	0.88	0.87
	2015	0.82	0.84	0.80	0.81
	2020	0.82	0.84	0.85	0.83
Kon Tum	2010	0.89	0.86	0.81	0.85
	2015	0.85	0.91	0.87	0.86
	2020	0.81	0.80	0.82	0.81
Dong Nai	2010	0.86	0.81	0.83	0.82
	2015	0.85	0.89	0.87	0.88
	2020	0.88	0.92	0.87	0.89

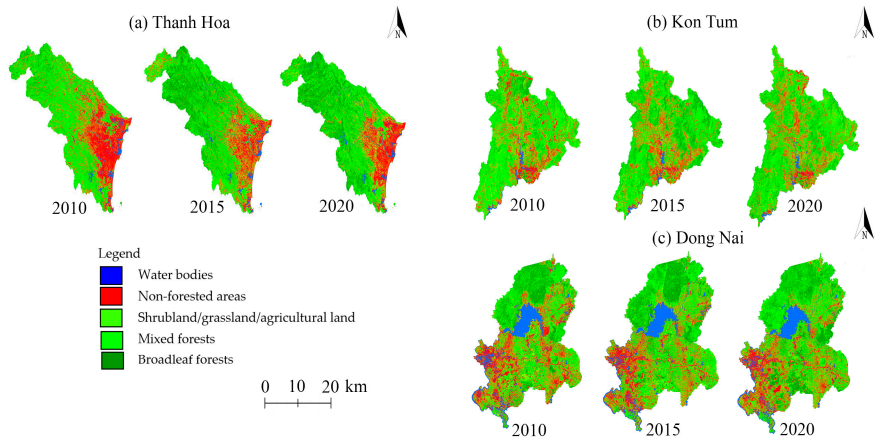


Figure 5. Land cover maps of study areas for 2010, 2015, and 2020.

Table 3. Dynamics of land cover categories in the study areas for the period 2010–2020.

Areas	Land Cover Categories	Area (ha)		
		2010	2015	2020
Thanh Hoa	water bodies	26,370	28,603	29,167
	non-forested areas	186,589	193,420	179,927
	shrubland/grassland/agricultural land	182,808	188,014	200,959
	mixed forests	535,691	475,539	430,246
	broadleaf forests	178,223	224,105	269,382
	Total	1,109,681	1,109,681	1,109,681
Kon Tum	water bodies	10,085	14,089	15,318
	non-forested areas	147,477	130,749	130,619
	shrubland/grassland/agricultural land	232,461	238,337	291,272
	mixed forests	445,438	443,458	424,937
	broadleaf forests	133,070	141,898	106,385
	Total	968,531	968,531	968,531
Dong Nai	water bodies	58,737	53,070	49,093
	non-forested areas	124,615	105,402	103,081
	shrubland/grassland/agricultural land	157,588	147,635	144,871
	mixed forests	169,496	188,758	190,128
	broadleaf forests	79,812	95,383	103,075
	Total	590,248	590,248	590,248

Based on the data presented in Table 3, in Thanh Hoa province, the area of broadleaf forests increased by 91,159 hectares (51.15%) over the ten-year period from 2010 to 2020, while the area of mixed forests decreased by 105,445 hectares (19.68%). This reduction in mixed forests was accompanied by an increase of 18,151 hectares (9.93%) in agricultural land, highlighting the recovery of ecologically valuable broadleaf forests alongside the expansion of agricultural activities. In Kon Tum province, the area of broadleaf forests decreased by 26,686 hectares (20.05%), while mixed forests declined by 20,501 hectares (4.60%). In contrast, the area of shrubland/grassland/agricultural land increased by 58,811 hectares (25.30%), indicating a significant shift from forested areas to agricultural land, as well as ongoing challenges related to illegal logging. The province's proximity to the borders with Laos and Cambodia further complicates forest conservation efforts. In Dong Nai province, the smallest of the three regions studied, broadleaf forests increased by 23,263 hectares (29.15%), and mixed forests expanded by 20,632 hectares (12.17%). Conversely, the area of shrubland/grassland/agricultural land decreased by 12,717 hectares (8.07%), and non-forested lands declined by 21,534 hectares (17.28%), reflecting the effectiveness of provincial policies and local initiatives aimed at conserving and restoring forest areas.

3.2. Forest Cover Changes Prediction Using the CA-Markov Model and the MOLUSCE Module

3.2.1. Prediction Results Using the CA-Markov Model

The first step involved constructing the transition matrix P, which defines the probabilities of transitions between land cover categories for the period 2010–2015, as shown in Figure 6. Using the CA-Markov model, area predictions are then generated for 2020, as shown in Table 4.

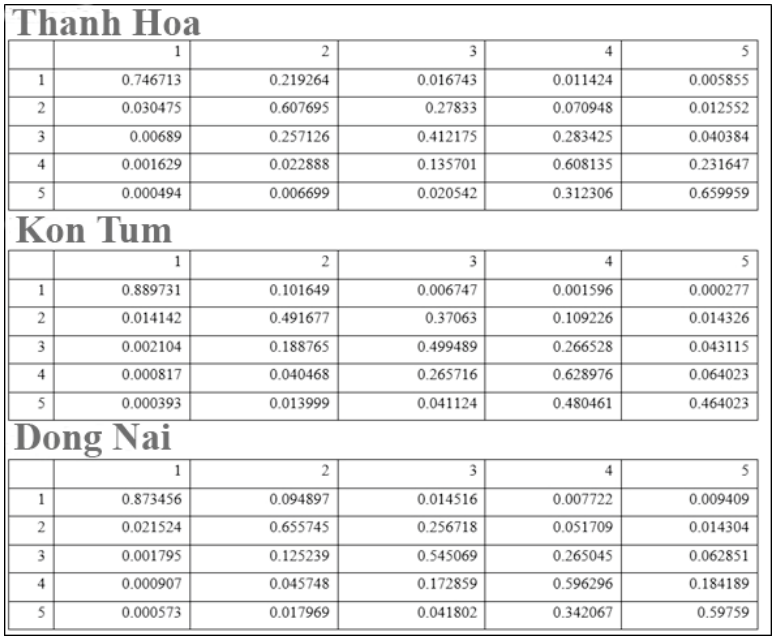


Figure 6. Land cover categories transition probability matrices for the period 2010–2015: 1—water bodies; 2—non-forested areas; 3—shrubland/grassland/agricultural land; 4—mixed forests; 5—broadleaf forests.

Table 4. Results of the area prediction using CA-Markov model for 2020.

Land Cover Categories	Area (ha)		
	Thanh Hoa	**Kon Tum**	**Dong Nai**
water bodies	71,087	29,579	57,204
non-forested areas	200,069	220,331	117,148
shrubland/grassland/agricultural land	262,116	288,020	148,833
mixed forests	355,485	356,780	162,160
broadleaf forests	317,497	267,344	134,569
Total	1,207,254	1,165,054	619,914
Deviation from actual areas, %	8.79	6.29	5.03

3.2.2. Prediction Results Using the MOLUSCE Module

The MOLUSCE module, utilizing an Artificial Neural Network (ANN) modeling approach, was applied to predict forest cover changes for the year 2020 based on training data from 2010 and 2015. The input variables incorporated into the ANN model included classified land cover maps, topographic factors (DEMs and slope), distance to roads, urban centers, and regional climatic variables (annual precipitation and temperature).

Following model training, the predicted land cover distribution for 2020 was generated and compared directly with the actual classified 2020 land cover maps. This comparative analysis allowed for a direct evaluation of the model's accuracy. Prediction accuracy was assessed using two methods. First, the overall deviation percentage between the predicted and actual 2020 areas of land cover categories was calculated for each province. The MOLUSCE module demonstrated low deviation rates: 1.61% for Thanh Hoa, 1.14% for Kon Tum, and 1.80% for Dong Nai (Table 5). These results indicate a high degree of agreement between the predicted and actual land cover distributions. Second, confusion matrices were generated to evaluate class-level prediction accuracy. From these matrices, the overall accuracy and the Kappa coefficient were calculated. The overall accuracy values exceeded

83% for all provinces, and Kappa coefficients ranged from 0.78 to 0.82, demonstrating a high degree of agreement according to standard interpretation thresholds.

Table 5. Results of the area prediction using MOLUSCE module for 2020.

Land Cover Categories	Area (ha)		
	Thanh Hoa	Kon Tum	Dong Nai
water bodies	32,123	28,447	60,123
non-forested areas	197,886	145,213	115,667
shrubland/grassland/agricultural land	189,335	287,334	152,290
mixed forests	405,687	420,333	167,443
broadleaf forests	266,753	98,257	105,329
Total	1,091,784	979,584	600,852
Deviation from actual areas, %	1.61	1.14	1.80

3.2.3. Comparison of Prediction Results Between the CA-Markov Model and the MOLUSCE Module

The comparative analysis between the CA-Markov model and the MOLUSCE module indicated substantial differences in predictive performance. The CA-Markov model, which relies on historical land cover transition probabilities, exhibited higher deviation rates when its 2020 predictions were compared with the actual classified maps. Specifically, overall deviation percentages of predicted land cover areas were 8.79% for Thanh Hoa, 6.29% for Kon Tum, and 5.03% for Dong Nai. These results indicate that while CA-Markov can capture general trends based on past transitions, it struggles to account for the dynamic environmental and anthropogenic factors influencing land cover changes. In contrast, the MOLUSCE module's ANN-based approach demonstrated significantly lower overall deviation percentages: 1.61% for Thanh Hoa, 1.14% for Kon Tum, and 1.80% for Dong Nai. The MOLUSCE module's performance can be attributed to its ability to incorporate multiple variables including topographic features (elevation, slope), infrastructure proximity (roads, urban centers), and climatic parameters (precipitation, temperature). Moreover, the ANN's capacity to model complex, nonlinear relationships between input variables and land cover transitions allowed for more accurate predictions.

Analysis of the deviation data presented in Table 6 clearly highlights the magnitude of the improvement achieved by using the MOLUSCE module. On average, the prediction deviations of the MOLUSCE module were approximately 5–7% lower than those of the CA-Markov model across the three provinces. This result confirms the advantage of integrating environmental and anthropogenic factors into land cover prediction models, especially in regions characterized by rapid land use changes and diverse ecological conditions.

Table 6. Land cover area prediction deviations by CA-Markov model and MOLUSCE module.

Objects	Land Cover Prediction Deviations by Different Methods (%)	
	CA-Markov Model	MOLUSCE Module
Thanh Hoa	8.79	1.61
Kon Tum	6.29	1.14
Dong Nai	5.03	1.8

3.3. Forest Cover Changes Prediction for 2025 and 2030 Using the MOLUSCE Module

Future land cover changes for 2025 and 2030 were simulated using the MOLUSCE module, building upon observed transitions from 2010 to 2020 and incorporating the environmental and anthropogenic variables within the ANN framework. The model

demonstrated high predictive reliability, as evidenced by its strong performance in validating 2020 projections (showing deviation rates below 2% across all study areas). This robust validation suggests that the 2025 and 2030 predictions maintain a high degree of accuracy. Projected land cover maps for each province are illustrated in Figure 7, and corresponding area statistics are presented in Table 7.

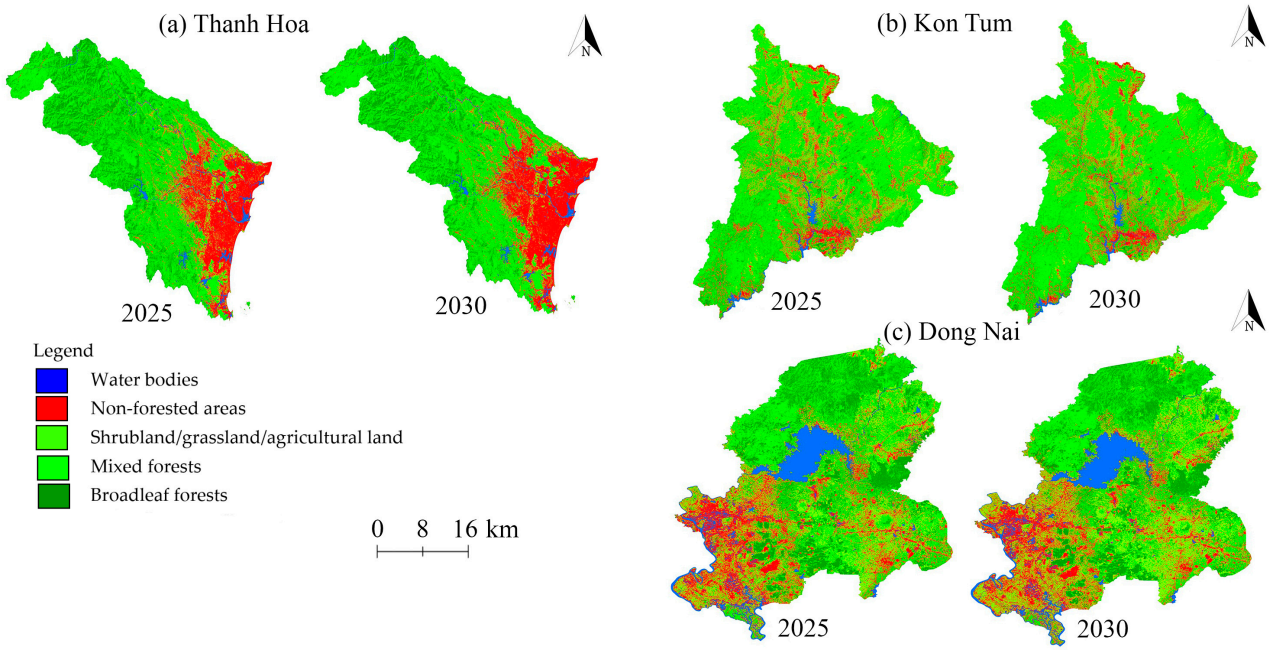


Figure 7. Predicted land cover maps for the study areas in 2025 and 2030.

Table 7. Predicted areas of land cover categories.

Land Cover Categories	Thanh Hoa		Kon Tum		Dong Nai	
	2025 (ha)	2030 (ha)	2025 (ha)	2030 (ha)	2025 (ha)	2030 (ha)
water bodies	29,456	28,244	16,238	16,402	48,167	47,680
non-forested areas	200,687	226,255	119,206	113,466	99,873	96,999
shrubland/grassland/agricultural land	174,199	139,814	266,689	242,123	166,657	181,157
mixed forests	449,904	475,737	476,266	510,838	159,368	142,175
broadleaf forests	255,435	239,631	90,132	85,702	116,183	122,237
Total	1,109,681	1,109,681	968,531	968,531	590,248	590,248

Based on the data presented in Table 7, and in comparison with the land cover in 2020, it is projected that during the period 2020–2030, Thanh Hoa province will experience a decrease in broadleaf forest area of 29,751 hectares (11.04%) and in shrubland/grassland/agricultural land of 61,145 hectares (30.43%). Meanwhile, the area of mixed forests is expected to increase by 45,491 hectares (10.57%), and non-forested lands by 46,328 hectares (25.75%). This indicates strong economic growth in Thanh Hoa during the projected period, driven by the ongoing construction of industrial facilities and infrastructure improvements to meet the province's development needs. At the same time, a shift in forest structure is observed, with mixed forests expanding at the expense of broadleaf forests, which contrasts with the previous 10-year trend. This transformation can be attributed to recent changes in provincial forestry policies and evolving national climate conditions. For Kon Tum province, it is expected that between 2020 and 2030, the area of broadleaf forests will decrease by 20,683 hectares (19.44%), while shrubland/grassland/agricultural land will decline by 49,149 hectares (16.87%). In contrast, mixed forests are projected to

increase by 85,901 hectares (20.21%). This suggests that the declining trend of broadleaf forests observed over the past decade will continue, while the dynamics of mixed forests and shrubland/grassland shift in the opposite direction compared with the previous period. According to our forecasts, the area of shrubland/grassland/agricultural land will continue to shrink, whereas the area of mixed forests will expand significantly. This change can be explained by the provincial government's policies on forest restoration, conservation, and protection, as well as the efforts by local communities to expand forested areas. These measures have begun to yield positive results in recent years, helping to restore forested land previously lost due to unauthorized land seizures and illegal logging for timber extraction. For Dong Nai province, it is expected that broadleaf forest area will increase by 19,162 hectares (18.59%), while shrubland/grassland/agricultural land will expand by 36,286 hectares (25.05%). In contrast, mixed forests are projected to decrease by 47,953 hectares (25.22%). This trend can be explained by policy changes in the Dong Nai provincial administration, which is actively preserving and expanding primary forests and national parks while also implementing land use restructuring. A portion of the forest land is being converted into agricultural land to align with the province's long-term economic development goals.

While direct validation data for the 2025 and 2030 projections are not yet available, the MOLUSCE module's performance for 2020 suggests that its predictions are reliable. These predictions provide valuable insights for forest management planning by identifying the areas most vulnerable to land cover transformation. Strengthened policy enforcement, expanded reforestation programs, and improved integration of conservation goals into local development plans could effectively counteract the anticipated deforestation trends, particularly in Thanh Hoa and Kon Tum provinces.

4. Discussion

4.1. Advantages of Remote Sensing and GIS Technology over Traditional Methods

The monitoring of forest cover changes in Vietnam is essential for conserving forest resources and addressing climate change challenges. Traditional methods of forest monitoring, primarily based on ground-based surveys, visual inspections, and manual cartographic techniques, have historically played an important role in forest resource assessment. However, these approaches present several inherent limitations that significantly affect the accuracy, timeliness, and comprehensiveness of forest cover monitoring, especially in topographically complex regions with challenging climatic conditions, such as Vietnam's diverse forest landscapes.

Firstly, field surveys are labor-intensive, time-consuming, and often logistically constrained by remote or mountainous terrain accessibility [28]. In Vietnam, where extensive forested regions are located in rugged uplands, physical access limitations frequently result in incomplete spatial coverage. Consequently, significant forest areas may be undersampled or entirely omitted, creating substantial biases in land cover estimates and preventing accurate documentation of localized forest cover changes. Secondly, traditional approaches face significant temporal limitations. Ground-based surveys are conducted infrequently due to their high cost and logistical challenges, making it difficult to detect rapid or seasonal changes in forest cover. This temporal infrequency creates substantial delays between actual land cover changes and their official documentation, reducing the relevance and responsiveness of forest management decisions [29]. Thirdly, manual observation and interpretation are inherently subjective and susceptible to human error. Variability in observer judgment, inconsistencies in measurement techniques, and difficulties in maintaining standardized criteria across different survey teams can all introduce errors and inconsistencies into forest monitoring datasets. These methodological weaknesses

prove particularly detrimental in ecologically diverse landscapes, where subtle differences between forest types or degradation levels may be overlooked or misclassified.

In contrast, remote sensing (RS) technology enables rapid and continuous data acquisition over forested areas, providing high-resolution satellite imagery and sensor data. This technology accurately identifies forest composition, coverage levels, and temporal changes, enhancing the objectivity, efficiency, and cost-effectiveness of land inventory processes. Additionally, GIS facilitates effective spatial data analysis and management, allowing users to create digital maps that model forest conditions and forecast trends [30].

4.2. Application of Remote Sensing and GIS in Assessing Forest Cover Changes

The application of RS and GIS technologies in this study proved essential for comprehensively assessing forest cover changes across three Vietnamese provinces: Thanh Hoa, Kon Tum, and Dong Nai, each with unique natural conditions. The integration of multi-temporal satellite imagery, environmental and anthropogenic variables allowed for the detailed mapping and analysis of forest dynamics over the decade from 2010 to 2020.

In Thanh Hoa province, characterized by both mountainous and lowland areas, RS facilitates large-scale monitoring of forest dynamics. GIS supports spatial data analysis and the creation of digital maps that clearly illustrate forest distribution and changes. Between 2010 and 2020, RS detected a 51.15% increase (91,159 ha) in broadleaf forests and a 19.68% decrease (105,445 ha) in mixed forests, with agricultural land increasing by 9.93% (18,151 ha). These trends reflect both ecological recovery and the expansion of agriculture. In Kon Tum province, which contains valuable primary forests, RS enables precise assessments of deforestation and agricultural encroachment. During the same period, broadleaf and mixed forests declined by 20.05% (26,685 ha) and 4.06% (20,501 ha), respectively, while shrubland, meadows, and agricultural land expanded by 25.30% (58,811 ha), indicating a shift in land use and ongoing pressures from illegal logging. In Dong Nai province, RS identified significant forest regeneration. Broadleaf forests expanded by 29.15% (23,263 ha), and mixed forests by 12.17% (20,632 ha), while shrubland/agricultural land and non-forested areas decreased by 8.07% (12,717 ha) and 17.28% (21,534 ha), respectively. These changes indicate the effectiveness of local forest restoration policies.

Human activities created significant pressure on forest ecosystems during the study period. Infrastructure development, agricultural expansion, and urbanization were key drivers of forest loss. The integration of distance to roads and urban centers layers into the classification and prediction models effectively captured these anthropogenic influences, illustrating that proximity to settlements was correlated with increased land cover transitions away from forested areas.

By enabling the integration and analysis of diverse datasets, RS and GIS technologies not only facilitated the accurate classification of forest cover but also allowed for the modeling of underlying drivers of change. This methodological approach directly supported this study's objectives: to improve forest cover classification accuracy and to enhance predictive modeling by considering both environmental and anthropogenic factors.

Ultimately, the findings confirm that RS and GIS provide powerful frameworks for detecting, understanding, and predicting forest cover dynamics. They also demonstrate that effective forest management and conservation strategies must account for both natural landscape characteristics and human development pressures, aligning with the broader goals of sustainable land use planning and biodiversity conservation.

4.3. Using the MOLUSCE Module to Predict Forest Cover Changes to 2030

The application of the MOLUSCE module, employing an Artificial Neural Network (ANN) approach, demonstrated substantial advantages over the CA-Markov model for

predicting forest cover changes to 2030 in the study areas. The superior performance of MOLUSCE was evident both in the higher predictive accuracy achieved for the 2020 validation year and in the model's ability to capture complex spatial patterns of land cover change.

One of the primary reasons for the MOLUSCE module's superiority lies in its methodological flexibility. While the CA-Markov model relies exclusively on historical transition probabilities and assumes stationary land cover change processes, MOLUSCE incorporates a wide range of supplementary variables that influence land use dynamics [31]. In this study, MOLUSCE integrated land cover maps and topographic factors (elevation, slope), infrastructure proximity (distance to roads and urban centers), and climatic variables (precipitation, temperature). This multi-variable approach allowed the model to account for both natural and anthropogenic impacts, leading to a more reliable projection of land cover changes.

Moreover, the ANN framework within MOLUSCE can identify and model complex nonlinear relationships between input features and land cover transitions [26]. This contrasts with the CA-Markov model's linear probabilistic assumptions, which tend to oversimplify the drivers of forest change, particularly in the heterogeneous environments of Vietnam. As a result, the MOLUSCE module achieved much lower deviation rates when predicting 2020 land cover distributions (approximately 1–2%), compared with the CA-Markov model's higher deviations (5–9%).

Thus, the MOLUSCE module was used for the 2030 projections. In Thanh Hoa province, broadleaf forests and shrubland/grassland/agricultural land are expected to decline (11.04% and 30.43%), while mixed forests and non-forested areas are expected to expand (10.57% and 25.75%) due to economic development and policy shifts. In Kon Tum, broadleaf forests and shrubland/grassland/agricultural land are projected to decrease by 19.44% and 16.87%, while mixed forests may rise by 20.21% due to restoration initiatives. In Dong Nai, increases of 18.59% (broadleaf forests) and 25.05% (shrubland/grassland/agricultural land) are expected, while mixed forests may decline by 25.22%, reflecting changing land use and the impact of protected areas.

4.4. Limitations and Recommendations for Future Research

While the methodologies applied in this study significantly improved the accuracy of forest cover classification and prediction, several limitations affecting result reliability should be acknowledged.

First, data limitations posed inherent challenges. Although the study integrated spectral, NDVI, topographic, and distance-based variables, the availability of high-resolution socio-economic and demographic data was limited [32]. Proxies such as distance to roads and urban centers were used to approximate human activity pressures. These proxies may not fully capture the complexities of land use decision making or the influence of local policy implementation. Additionally, climatic data derived from global datasets (WorldClim) at approximately 1 km spatial resolution may overlook finer-scale climatic variations that influence forest cover changes.

Second, the temporal resolution of remote sensing data is a limitation [33]. The study relied on five-year intervals (starting in 2010, 2015, and 2020) for land cover data due to cloud cover limitations and data availability. More frequent observations could capture short-term dynamics and better distinguish between temporary and permanent land cover changes.

Third, limitations related to the modeling approaches must be noted. Although the ANN-based MOLUSCE module outperformed the CA-Markov model in predictive

accuracy, it remains a "black-box" system, providing limited insight into the model operation [34].

To address these limitations, several recommendations can be made for future research. First, incorporating more detailed socio-economic data—including land ownership, land use regulations, economic activity, and population dynamics at finer spatial resolutions—would significantly improve modeling of anthropogenic drivers. Second, utilizing higher temporal resolution remote sensing datasets, like annual Sentinel-2 imagery, could improve the detection of forest cover changes. Third, adopting explainable AI techniques such as feature importance analysis or interpretable neural network architectures would provide crucial insights into the variable contributions on forest cover transitions and enhance model transparency [35]. Fourth, the systematic integration of ground truth data through field validation and local knowledge would strengthen the reliability of remote sensing interpretations.

Implementing these improvements would advance the accuracy, transparency, and policy relevance of forest monitoring systems, ultimately supporting more effective sustainable land management strategies not only in Vietnam but also in other countries facing similar challenges.

5. Conclusions

This study employs a remote sensing approach integrated with GIS technology to monitor forest cover changes in Vietnam, providing valuable insights for scientific research and practical applications in forest management, conservation, and restoration at local, regional, and global scales. This integrated approach enables a comprehensive analysis of forest land dynamics and their interactions with environmental factors. This research focuses on three key provinces in northern, central, and southern Vietnam, each characterized by distinct climatic, topographic, and anthropogenic conditions. By incorporating diverse data sources, including multi-temporal satellite images, NDVI indices, topographic and climatic variables, infrastructure proximity, and applying advanced classification and prediction approaches (Random Forest algorithm, CA-Markov model, and ANN-based MOLUSCE module), this research achieved high classification accuracies and reliable predictions of future land cover dynamics. The results reveal significant shifts in forest land categories across Thanh Hoa, Kon Tum, and Dong Nai provinces. In Thanh Hoa, broadleaf forest recovery coincides with agricultural expansion, while Kon Tum experiences continued deforestation due to illegal logging and agricultural conversion. In contrast, Dong Nai shows successful forest restoration, largely attributed to effective local policies. These findings underscore the varying impacts of agricultural activity, deforestation, and reforestation efforts on forest cover. Projections indicate continued declines in certain forest types and further conversion to agricultural and other land uses by 2030. The integration of RS and GIS technologies provides substantial advantages for forest monitoring. RS enables consistent, large-scale observations of forest dynamics, overcoming the spatial and temporal limitations of traditional ground-based methods. GIS platforms facilitate the combination of remote sensing data with supplementary spatial information, enhancing the understanding of land cover change drivers and enabling more precise spatial analysis and modeling. The application of RS and GIS technologies directly supports sustainable forest resource management by providing timely, accurate geospatial data that enables decision makers to identify deforestation risks, prioritize conservation areas, evaluate policy effectiveness, and develop proactive management strategies. By analyzing current patterns and predicting future trends, this study supports land management and planning initiatives, contributing to the development of sustainable strategies for the conservation, restoration, and sustainable use of Vietnam's forest land resources.

Author Contributions: Conceptualization, V.K. and A.N.; methodology, V.K.; software, A.N.; validation, C.P.; formal analysis, A.N.; investigation, C.P.; resources, A.N.; data curation, C.P.; writing—original draft preparation, A.N. and V.K.; writing—review and editing, V.K., A.N. and C.P.; visualization, A.N. All authors have read and agreed to the published version of the manuscript.

Funding: This research received no external funding.

Data Availability Statement: The data presented in this study are available on request from the corresponding author.

Conflicts of Interest: The authors declare no conflicts of interest.

References

1. Bykowa, E.; Banikevich, T.; Zalivatskaya, N.; Pirogova, O. Modeling the Cadastral Value of Land Plots of Gardening and Horticultural Non-Profit Partnerships Taking into Account the Influence of Local Factors of the Territory. *Land* **2024**, *13*, 1004. [CrossRef]
2. Skachkova, M.; Guryeva, O. Monitoring of the State of Saint Petersburg Green Spaces by Remote Sensing Data. *Ecol. Ind. Russ.* **2023**, *27*, 51–57. [CrossRef]
3. Skachkova, M.E. Urban green infrastructure assessment: Identification of public green spaces misuse. *Geogr. Environ. Sustain.* **2024**, *17*, 183–197. [CrossRef]
4. Banikevich, T.D.; Bykowa, E.N.; Zalivatskaya, N.V.; Pirogova, O.E. Pattern determination of the territory local factors influence on the land plots' cadastral value of gardening and horticultural non-profit partnerships. *Popul. Econ.* **2024**, *8*, 86–107. [CrossRef]
5. Chinh, L.; Binh, T.P.; Tran, V.P.; Costache, R.; Nguyen, H.D.; Amiri, M.; Bui, Q.D.; Nguyen, L.T.; Van Le, H.; Prakash, I.; et al. GIS-Based ensemble computational models for flood susceptibility prediction in the Quang Binh Province, Vietnam. *J. Hydrol.* **2021**, *599*, 126500.
6. Duong, B.V.; Fomenko, I.K.; Nguyen, K.T.; Zerkal, O.V.; Sirotkina, O.N.; Vu, D.H. Landslide hazard assessment in Tinh Tuc town, Cao Bang province, Vietnam using Frequency ratio method and the combined Fractal-frequency ratio method. *J. Min. Inst.* **2024**, *268*, 613–624.
7. Kovyazin, V.; Bogdanova, E. Current State of Specially Protected Natural Areas of the Arctic of the Russian Federation. *Ecol. Ind. Russ.* **2025**, *29*, 59–65.
8. Xu, Z.; Man, X.; Cai, T.; Shang, Y. How Potential Evapotranspiration Regulates the Response of Canopy Transpiration to Soil Moisture and Leaf Area Index of the Boreal Larch Forest in China. *Forests* **2022**, *13*, 571. [CrossRef]
9. Kornilov, Y.N.; Romanchikov, A.Y.; Anikeeva, A.A. Estimating deformation process through single shot close range photogrammetry method in Agisoft Metashape. *Geod. Cartogr.* **2023**, *84*, 2–11. [CrossRef]
10. Valkov, V.A.; Vinogradov, K.P.; Mustafin, M.G.; Valkova, E.O. Creating highly informative rasters based on laser scanning and aerial photography data. *Geod. Cartogr.* **2022**, *83*, 40–49. [CrossRef]
11. Smirnyakov, V.V.; Rodionov, V.A.; Smirnyakova, V.V.; Orlov, F.A. The influence of the shape and size of dust fractions on their distribution and accumulation in mine workings when changing the structure of air flow. *J. Min. Inst.* **2022**, *253*, 71–81. [CrossRef]
12. Lapinskas, A.A. Influence of mining rent on the efficiency of using natural potential: The paradox of plenty and its Russian specifics. *J. Min. Inst.* **2023**, *259*, 79–94. [CrossRef]
13. Yermolayev, O.; Platoncheva, E.; Essuman, Q.B. Spatial-Temporal Dynamics of the Ephemeral Gully Belt on the Plowed Slopes of River Basins in Natural and Anthropogenic Landscapes of the East of the Russian Plain. *Geosciences* **2020**, *10*, 167. [CrossRef]
14. Guimarães, N.; Pádua, L.; Marques, P.; Silva, N.; Peres, E.; Sousa, J.J. Forestry Remote Sensing from Unmanned Aerial Vehicles: A Review Focusing on the Data, Processing and Potentialities. *Remote Sens.* **2020**, *12*, 1046. [CrossRef]
15. Zhang, M.; Chen, E.; Zhang, C.; Liu, C.; Li, J. Multi-Scenario Simulation of Land Use Change and Ecosystem Service Value Based on the Markov–FLUS Model in Ezhou City, China. *Sustainability* **2024**, *16*, 6237. [CrossRef]
16. Elias, R.C.; Celso, A.G.S.; Richarde, M.S.; Bacani, V.M.; Pott, A. Future scenarios based on a CA-Markov land use and land cover simulation model for a tropical humid basin in the Cerrado/Atlantic forest ecotone of Brazil. *Land Use Policy* **2021**, *101*, 105141.
17. Wu, X.; He, H.; Zhang, L.; Feng, L.; Ren, X.; Liu, W.; Zou, C.; Lin, N. Spatial sampling design optimization of monitoring network for terrestrial ecosystem in China. *Sci. Total Environ.* **2022**, *847*, 57397. [CrossRef]
18. Kıvanç, Y.; Neşe, G.; Abdullah, E.; Gülci, S. Evaluation of eco-friendly soil slope stabilization techniques for forest roads by using an Artificial Neural Network (ANN). *Int. J. Sediment Res.* 2025, *in press*.
19. Dang, H.N.; Nguyen, V.T.; Tran, D.L.; Ha, N.M.; Nghi, D.T.; Ha, T.M.; Hao, D.M.; Van Chien, N.; Thanh, T.D. Enrichment and distribution of metals in surface sediments of the Thanh Hoa coastal area, Viet Nam. *Reg. Stud. Mar. Sci.* **2021**, *41*, 101574.
20. Paudyal, K.; Samsudin, Y.B.; Baral, H.; Okarda, B.; Phuong, V.T.; Paudel, S.; Keenan, R.J. Spatial Assessment of Ecosystem Services from Planted Forests in Central Vietnam. *Forests* **2020**, *11*, 822. [CrossRef]

21. The, V.P.; Tuyet, A.T.; Hau, D.T.; Do, A.N.T. Assessing groundwater potential for mitigating salinity issues in agricultural areas of southern Dong Nai province, Vietnam. *Groundw. Sustain. Dev.* **2024**, *25*, 101177.
22. Zhou, L.; Zhou, W.; Chen, J.; Xu, X.; Wang, Y.; Zhuang, J.; Chi, Y. Land surface phenology detections from multi-source remote sensing indices capturing canopy photosynthesis phenology across major land cover types in the Northern Hemisphere. *Ecol. Indic.* **2022**, *135*, 108579. [CrossRef]
23. Peng, D.; Zhang, H.; Yu, L.; Wu, M.; Wang, F.; Huang, W.; Liu, L.; Sun, R.; Li, C.; Wang, D.; et al. Assessing spectral indices to estimate the fraction of photosynthetically active radiation absorbed by the vegetation canopy. *Int. J. Remote Sens.* **2018**, *39*, 8022–8040. [CrossRef]
24. Huang, Z.; Du, H.; Li, X.; Zhang, M.; Mao, F.; Zhu, D.E.; He, S.; Liu, H. Spatiotemporal LUCC Simulation under Different RCP Scenarios Based on the BPNN_CA_Markov Model: A Case Study of Bamboo Forest in Anji County. *ISPRS Int. J. Geo-Inf.* **2020**, *9*, 718. [CrossRef]
25. Yulianto, F.; Maulana, T.; Khomarudin, M.R. Analysis of the dynamics of land use change and its prediction based on the integration of remotely sensed data and CA-Markov model, in the upstream Citarum Watershed, West Java, Indonesia. *Int. J. Digit. Earth* **2018**, *12*, 1151–1176. [CrossRef]
26. Jiang, G.; Zheng, Q. Remote Sensing Recognition and Classification of Forest Vegetation Based on Image Feature Depth Learning. *Mob. Inf. Syst.* **2022**, *2022*, 9548552. [CrossRef]
27. Zahid, A.; Dashtipour, K.; Abbas, H.; Mabrouk, I.B.; Al-Hasan, M.; Ren, A.; Imran, M.A.; Alomainy, A.; Abbasi, Q.H. Machine learning enabled identification and real-time prediction of living plants' stress using terahertz waves. *Def. Technol.* **2022**, *18*, 1330–1339. [CrossRef]
28. Gunathilaka, R.P.D.; James, C.R.S.; Christopher, M.F. Adaptation to climate change in perennial cropping systems: Options, barriers and policy implications. *Environ. Sci. Policy* **2018**, *82*, 108–116. [CrossRef]
29. Pérez-Romero, J.; González-Sanchis, M.; Blanco-Cano, L.; Del Campo, A.D. Development of a multi-objective decision support system for eco-hydrological forest management that quantifies and optimizes ecosystem services related to Carbon, Water, Fire-risk and Eco-resilience (CAFE). *J. Environ. Manag.* **2025**, *380*, 125103. [CrossRef]
30. Narayan, K.; Khanindra, P.; Abhisek, C.; Singh, C.P.; Chowdary, V.M.; Kumar, S.; Sahoo, S. Forest health assessment for geo-environmental planning and management in hilltop mining areas using Hyperion and Landsat data. *Ecol. Indic.* **2019**, *106*, 105471.
31. Omar, S.; Rajan, G.; Ayyoob, S. Predicting Prayagraj's Urbanization Trajectory using CA-ANN Modelling: Population Pressures and Land Use Dynamics. *J. Environ. Manag.* **2024**, *370*, 122469.
32. Matrokhina, K.V.; Trofimets, V.Y.; Mazakov, E.B.; Makhovikov, A.B.; Khaykin, M.M. Development of methodology for scenario analysis of investment projects of enterprises of the mineral resource complex. *J. Min. Inst.* **2023**, *259*, 112–124. [CrossRef]
33. Hartley, R.J.L.; Leonardo, E.M.; Massam, P.; Watt, M.S.; Estarija, H.J.; Wright, L.; Melia, N.; Pearse, G.D. An Assessment of High-Density UAV Point Clouds for the Measurement of Young Forestry Trials. *Remote Sens.* **2020**, *12*, 4039. [CrossRef]
34. Hu, Y.; Qin, L.; Li, S.; Li, X.; Zhou, R.; Li, Y.; Sheng, W. Adaptive corrected parameters algorithm applied in cooling load prediction based on black-box model: A case study for subway station. *Energy Build.* **2023**, *297*, 113429. [CrossRef]
35. Amreen, B.; Yung, B. A lightweight multi-path convolutional neural network architecture using optimal features selection for multiclass classification of brain tumor using magnetic resonance images. *Results Eng.* **2025**, *25*, 104327.

Disclaimer/Publisher's Note: The statements, opinions and data contained in all publications are solely those of the individual author(s) and contributor(s) and not of MDPI and/or the editor(s). MDPI and/or the editor(s) disclaim responsibility for any injury to people or property resulting from any ideas, methods, instructions or products referred to in the content.